Available online at www.sciencedirect.com
SCIENCE DIRECT
Journal of Catalysis 237 (2006) 58–66
JOURNAL OF CATALYSIS
www.elsevier.com/locate/jcat

Effect of vanadium substitution in the cesium salts of Keggin-type heteropolyacids on propane partial oxidation

Xiu-Kai Li [a], Jing Zhao [a], Wei-Jie Ji [a,*], Zhi-Bing Zhang [a], Yi Chen [a], Chak-Tong Au [b,*], Scott Han [c], Hartmut Hibst [d]

[a] *Key Laboratory of Mesoscopic Chemistry, MOE, Department of Chemistry, Nanjing University, Nanjing 210093, China*
[b] *Department of Chemistry, Center for Surface Analysis and Research, Hong Kong Baptist University, Kowloon Tong, Hong Kong, China*
[c] *Rohm & Haas Company, Philadelphia, PA 19106-2399, USA*
[d] *BASF Aktiengesellschaft, 67056 Ludwigshafen, Germany*

Received 23 August 2005; revised 19 October 2005; accepted 20 October 2005

Available online 18 November 2005

Abstract

The catalytic behavior of the cesium salts of heteropolyacids with vanadium species substituted at the primary and/or secondary structure of Keggin oxoanions was systematically studied for propane partial oxidation. The physicochemical properties of the samples were explored by FTIR, UV–visible diffuse reflectance spectroscopy, XRD, and TPR techniques. The introduction of vanadium species to the primary structure of heteropoly compounds (HPCs) resulted in enhanced catalytic activity; with time on stream, a small fraction of vanadium species could be segregated from the oxoanion. When vanadium species was introduced to the secondary structure of HPCs, activity and selectivity to acrylic acid (AA) were notably enhanced. It is deduced that a small amount of vanadium species at the secondary structure of Keggin-type HPCs could interact synergistically with the oxoanion and cesium entities, inducing a positive effect on propane oxidation to AA as a result. The highest AA yield was observed over the $H_{0.1}Cs_{2.5}(VO)_{0.2}PMo_{12}O_{40}$ catalyst. The effect of operation variables on catalyst performance was also investigated, and it was found that the $H_{0.1}Cs_{2.5}(VO)_{0.2}PMo_{12}O_{40}$ catalyst was efficient in both oxygen-rich and hydrocarbon-rich atmospheres, and that the presence of steam can considerably suppress the formation of carbon oxides.

Keywords: Vanadium species; Heteropoly compounds; Propane oxidation; Acrylic acid

1. Introduction

Due to the unique acidic and redox properties of heteropoly compounds (HPCs), these materials with Keggin structure have been intensively studied as oxidation catalysts for both heterogeneous and homogeneous processes [1–3]. In heterogeneous applications, HPCs have been widely used to catalyze the oxidative dehydrogenation of alkanes, such as propane to propylene and ethane to ethylene [4,5]. Recently, HPCs have drawn increased attention as catalysts for one-step conversion of low alkanes into value-added oxygenated products, for example, oxidation of *iso*-butane to methacrylic acid (MAA) [6–8], oxidation of *n*-butane to maleic anhydride [9,10], and partial oxidation of propylene/propane to acrylic acid (AA) [11–17].

Three types of catalysts have been studied for the production of AA via one-step propane oxidation: HPCs, vanadyl pyrophosphates (VPOs), and mixed metal oxides (MMOs). The common features of an active catalyst are the presence of vanadium as well as appropriate redox and acidic characteristics [18]. As for HPCs used in heterogeneous oxidation, vanadium is usually introduced into the oxoanions by replacing one or more of the molybdenum atoms. Centi et al. [19] reported that the substituted framework of $H_5PMo_{10}V_2O_{40}$ showed reasonable initial activity and selectivity, but the catalyst deactivated quickly within 1.5 h due to decomposition of the oxoanion Keggin structure. In heteropolyacids (HPAs), substitution of proton with alkali and/or transition metal elements showed improved activity and thermal stability. Mizuno et al. [20] re-

* Corresponding authors.
E-mail addresses: jiwj@nju.edu.cn (W.-J. Ji), pctau@hkbu.edu.hk (C.-T. Au).

0021-9517/$ – see front matter
doi:10.1016/j.jcat.2005.10.022

ported that 13% AA yield was obtained over an iron-containing $H_{1.26}Cs_{2.5}Fe_{0.08}PMo_{11}VO_{40}$ catalyst at 380 °C, and segregation of vanadium entities from the oxoanion structure was observed at 500 °C. In another study, the $H_{1.5}Cs_{2.5}PMo_{11}VO_{40}$ catalyst produced only trace amounts of AA [21]. An AA yield of 10.2% was reportedly achieved over molybdophosphoric acid supported on a polyoxometallate salt with certain amount of vanadium located in the secondary structure [22]. The presence of vanadium species also showed a notable impact on the partial oxidation of *n*-butane. It has been generally recognized that HPCs lacking a vanadium component are rather inactive for *n*-butane oxidation [10].

It seems that it is important to clarify the role of vanadium species located in the primary and secondary structures in alkane oxidation. Casarini et al. [9] studied the effect of vanadium in the primary and secondary structures of HPAs on *n*-butane oxidation. However, to date there has been no report on the vanadium species existing in the primary and/or secondary structure for propane oxidation, and no clear documentation on the catalytic behavior of the related materials. In this study, we purposely introduced vanadium species into the primary (Keggin anion) and/or the secondary structure of the cesium salts of HPAs to investigate their behaviors in propane partial oxidation.

2. Experimental

2.1. Catalyst preparation

The HPAs (AR grade) with or without vanadium substitution at the primary structure were purchased from Inorganic Colour and Chemical, Japan, which verified the chemical composition and stoichiometry of the samples. The received HPAs were further purified via ether extraction and water recrystallization. The crystals were filtered out and dried at 50 °C overnight and then left at 120 °C for 8–10 h. The dried solids were stored in a desiccator for later use. The cesium salts of HPAs were prepared via the reaction of purified HPAs with an appropriate amount of cesium carbonate in aqueous solution.

To introduce vanadium into the secondary structure of HPCs, an aqueous solution of $VOCl_2$ was first prepared by reacting V_2O_5 with an appropriate amount of hydrochloric acid at 70 °C for 6 h. Then the resulting dark-blue solution was cooled to room temperature (RT) and diluted to 0.1 mol L^{-1} for use. All HPC samples containing vanadium at the secondary structure [$(VO)^{2+}$ as the counter ions] were prepared by the precipitation method. For example, the typical procedure for preparing $H_{0.1}Cs_{2.5}(VO)_{0.2}PMo_{12}O_{40}$ was as follows: First, 3.0 g of $H_3PMo_{12}O_{40}$ was dissolved in 28 mL of distilled water at 50 °C under stirring. Then 3.28 mL of aqueous solution of $VOCl_2$ (0.1 mol L^{-1}) was added slowly, followed by 21.8 mL of aqueous solution of Cs_2CO_3 (0.15 mol L^{-1}) added dropwise at a rate of 1–2 mL min^{-1}. The resulting suspension was evaporated to dryness at 50 °C, then kept at 120 °C in air for 8–10 h. The resulting yellow powder was pressed, crushed, and sieved to 20–40 mesh for use.

2.2. Catalyst characterization

The freshly prepared samples, as well as a number of selected used catalysts, were characterized by various techniques. For the used samples, they were subject to reactions of continuous running in the temperature range of 350–430 °C for >10 h at a feed composition of $C_3/O_2/He$ (v/v/v) = 10/20/70. FTIR spectra of the catalysts were obtained using a NEXUS-870 FTIR spectrometer at RT by the KBr method. Surface areas of the samples were measured by the BET method (N_2 adsorption) with an ASAP2000 instrument. Phase composition of the samples were identified by powder X-ray diffraction (Philips X' Pert Pro, Cu-K_α radiation) in the 2θ range of 5–60°. UV–visible diffuse reflectance spectra were recorded at RT using a Shimadzu UV-2401PC UV–vis spectrometer with barium sulfate as the reference sample. Temperature-programmed reduction (TPR) was carried out in the temperature range of RT–1000 °C. The sample (50 mg) was reduced in a feed of 5% H_2/N_2 (40 mL min^{-1}) at a heating rate of 5 °C min^{-1}.

2.3. Reaction study

Propane oxidation was carried out under atmospheric pressure in a conventional fixed-bed Pyrex tubular reactor (Φ = 6 mm) in a temperature range of 360–430 °C. The feed composition was $C_3/O_2/He$ (v/v/v) = 17/30/53 or $C_3/O_2/He$ (v/v/v) = 10/20/70, and the gas hourly space velocity was 900 h^{-1}. Before the reaction, 1 g of as-prepared catalyst was diluted with 1 g of quartz chips to prevent the generation of hot spots during the reaction, then pretreated in N_2 stream (60 mL min^{-1}) at 300 °C for 1 h, to remove adsorbed water. The reactant was fed through a mass flow controller. The products were analyzed with an on-line gas chromatograph system using a HP FFAP capillary column for propane and oxygenate separation; a packed Hayesep D HP column for O_2(CO), CO_2, $C_3^=$, and C_3 separation; and a packed 5A molecular sieve column for O_2 and CO separation. The data were collected after the reaction had been stabilized at a desired temperature; the carbon balance usually exceeded 92%.

3. Results and discussion

3.1. Characterization

3.1.1. FTIR spectroscopy

The HPC samples (free acids and cesium salts) exhibited four characteristic IR bands at 1054–1064, 954–961, 860–880, and 740–790 cm^{-1}, attributable to $\nu_{as\,P–Oi}$, $\nu_{s\,Mo=Ot}$, $\nu_{s\,Mo–Ob–Mo}$, and $\nu_{s\,Mo–Oc–Mo}$, respectively [9,21,23]. With a V atom substituting for Mo in the primary structure of oxoanion, the P–O and Mo=O bands shifted toward lower wavenumbers and shoulders appeared at 1080 and 996 cm^{-1}, due to a reduced structure symmetry [9,21].

Fig. 1 shows the IR spectra of the used catalysts. The IR bands characteristic of Keggin oxoanions were essentially retained for all of the samples, indicating that they were rather stable under those reaction conditions. Note that a minor band at

$\sim$1033 cm^{-1} is observed over the $H_{1.5}Cs_{2.5}PMo_{11}VO_{40}$, $H_{1.1}Cs_{2.5}(VO)_{0.2}PMo_{11}VO_{40}$, and $H_{0.5-2x}Cs_{2.5}(VO)_xPMo_{12}O_{40}$ ($x \geqslant 0.2$) catalysts. Moreover, the bands (at $\sim$1033 cm^{-1}) of $H_{1.5}Cs_{2.5}PMo_{11}VO_{40}$ and $H_{1.1}Cs_{2.5}(VO)_{0.2}PMo_{11}VO_{40}$ are more intense than the band of $H_{0.5-2x}Cs_{2.5}(VO)_xPMo_{12}O_{40}$ ($x \geqslant 0.2$). This minor band can be ascribed to the band of $\nu_{V=O}$ in free V_2O_5, indicating that a small fraction of V species has segregated from the structure of the V-containing HPCs [20]. Also note the changed IR spectra of the used $H_{1.5}Cs_{2.5}PMo_{11}VO_{40}$ and $H_{1.1}Cs_{2.5}(VO)_{0.2}PMo_{11}VO_{40}$ catalysts. The ν_{P-O} and $\nu_{Mo=O}$ bands shifted slightly to $\sim$1062 and 964 cm^{-1}, close to the band of $H_{0.5-2x}Cs_{2.5}(VO)_xPMo_{12}O_{40}$ ($x = 0$–0.25), and the shoulders at 1080 and 996 cm^{-1} almost disappeared, signifying the segregation of vanadium species from the primary structure of oxoanions, possibly as a result of partial reduction/decomposition of Keggin structure during the reaction.

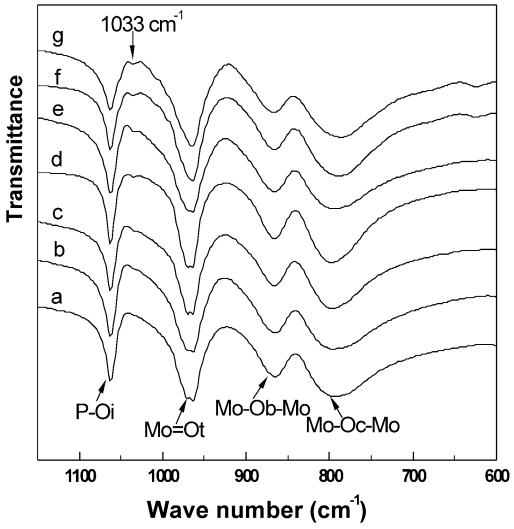

Fig. 1. Infrared spectra of the samples after reactions (feed composition: C_3/O_2/He (v/v/v) = 10/20/70; reaction temperature: 350–430 °C; time on stream: >10 h). (a–e) $H_{0.5-2x}Cs_{2.5}(VO)_xPMo_{12}O_{40}$ (x = 0–0.25); (f) $H_{1.5}Cs_{2.5}PMo_{11}VO_{40}$; (g) $H_{1.1}Cs_{2.5}(VO)_{0.2}PMo_{11}VO_{40}$.

The foregoing observations suggest that the vanadium species can partially segregate from the structure of the cesium salts of HPCs during the reactions, and that the segregation originates mainly from the primary structure. Similar phenomenon has been observed over other Keggin-type HPCs during propane oxidation [16,17,19,21]. It was found that the stability of vanadium species in the oxoanion increased with increasing Cs^+ substitution to protons in the secondary structure [17]. Accompanying the partial disintegration of oxoanion structure, some free molybdenum oxide species could have been formed. However, because of the heavy overlapping of the IR band of free molybdenum oxide with that of Mo species in oxoanion, the former could have hardly been observed in IR investigations.

3.1.2. UV–visible diffuse reflectance spectroscopy

Fig. 2 shows the UV–visible diffuse reflectance spectra of the samples before (A) and after (B) reaction. In the fresh samples, the ligand-metal charge transfer (LMCT) bands of Mo^{6+}–O^{2-} (in octahedral coordination) were observed at ca. 280–370 nm. The band in the 700–900 nm range can be ascribed to an intervalence charge-transfer transition (e.g., Mo^{5+}–Mo^{6+}) and indicates the presence of octahedral Mo^{5+} originating from the dehydrogenation and partial reduction of heteropoly anions during heat treatment [24]. In used samples the spectrum profiles basically remained unchanged, except for an increased intensity of the band in the 700–900 nm region as a result of further oxoanion reduction, as is consistent with the color changes before and after reaction (see Section 3.2.1).

It should be noted that additional unresolved bands centered at around 480–520 nm were observed over $H_{1.5}Cs_{2.5}PMo_{11}VO_{40}$ and $H_{1.1}Cs_{2.5}(VO)_{0.2}PMo_{11}VO_{40}$ before reaction; these were attributed to the presence of vanadium in the oxoanions [9]. After reaction, the related bands almost disappeared, and the spectra became similar to those of $H_{0.5}Cs_{2.5}PMo_{12}O_{40}$ and $H_{0.1}Cs_{2.5}(VO)_{0.2}PMo_{12}O_{40}$, providing more evidence supporting the partial segregation of vanadium from the primary structure of oxoanion.

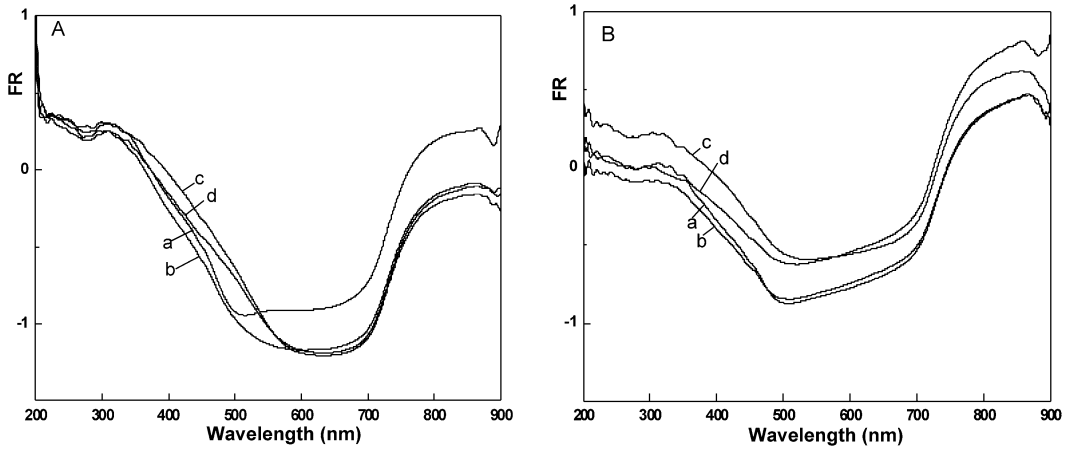

Fig. 2. UV–visible diffuse reflectance spectra of the samples (A) before and (B) after reaction. (a) $H_{0.5}Cs_{2.5}PMo_{12}O_{40}$; (b) $H_{0.1}(VO)_{0.2}Cs_{2.5}PMo_{12}O_{40}$; (c) $H_{1.5}Cs_{2.5}PMo_{11}VO_{40}$ and (d) $H_{1.1}Cs_{2.5}(VO)_{0.2}PMo_{11}VO_{40}$.

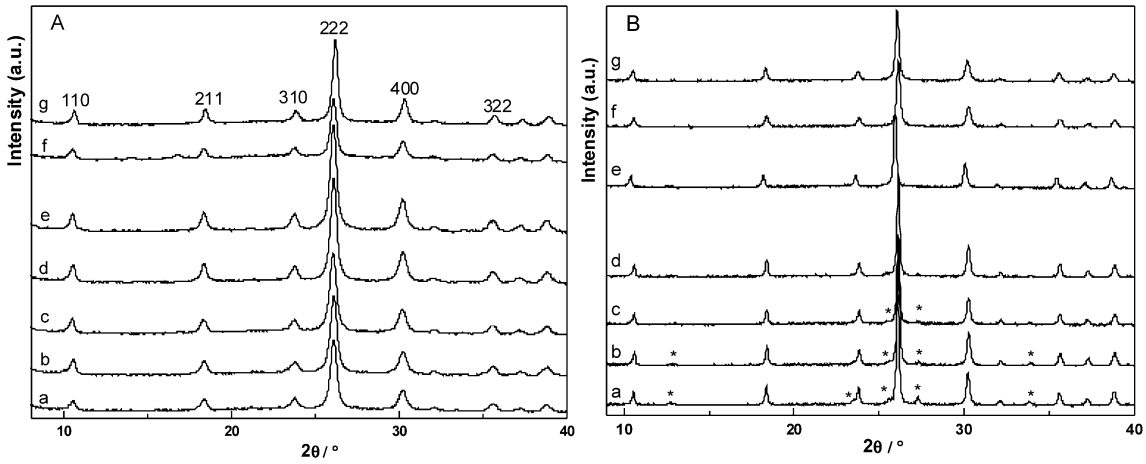

Fig. 3. X-Ray diffraction patterns of the samples (A) before and (B) after reaction. (a–e) $H_{0.5-2x}Cs_{2.5}(VO)_xPMo_{12}O_{40}$ ($x = 0$–0.25); (f) $H_{1.5}Cs_{2.5}PMo_{11}VO_{40}$ and (g) $H_{1.1}Cs_{2.5}(VO)_{0.2}PMo_{11}VO_{40}$. * α-MoO_3 phase.

3.1.3. XRD

To investigate the phase composition as well as the structural stability of the HPC catalysts, XRD data were collected over the fresh and the used samples; the results are shown in Fig. 3. For all of the samples, the main XRD lines were at $2\theta = 10.5°$, 18.3°, 23.7°, 26.1°, 30.2°, 35.6°, and 38.8°, which are commonly assigned to cubic alkaline salts of HPA (in our case the Cs^+-substituted HPCs) [25]. The intensity of diffraction patterns for the serial samples of $H_{0.5-2x}Cs_{2.5}(VO)_xPMo_{12}O_{40}$ strengthened gradually with increasing vanadium content; a similar phenomenon was also observed over $H_{1.1}Cs_{2.5}(VO)_{0.2}PMo_{11}VO_{40}$ and $H_{1.5}Cs_{2.5}PMo_{11}VO_{40}$. Therefore, the VO^{2+} species at the secondary structure of HPCs exhibited function similar to that of alkaline metals, and, consequently, the salt feature of the catalysts was enhanced.

Fig. 3B shows the XRD patterns of the used samples. Another phase with 2θ diffraction lines at 12.8°, 23.5°, 25.6°, 27.3°, and 33.9° was detected in the $H_{0.5-2x}Cs_{2.5}(VO)_xPMo_{12}O_{40}$ sample series ($x = 0$–0.15); this can be assigned to the α-MoO_3 phase. This indicates that the Keggin structure of oxoanion can partially disintegrate, as revealed by the results of IR investigation. The free vanadium oxide phase can hardly be detected from the XRD patterns, probably due to the low content and/or small dimensions of the entities. (IR is more sensitive in detecting the segregated vanadium oxide species, see the spectra of Fig. 1.) In addition, the intensity of diffraction patterns of α-MoO_3 phase diminished with increasing vanadium substitution at the secondary structure, and the α-MoO_3 phase was not detected at higher vanadium content ($x \geqslant 0.2$). On the other hand, both $H_{1.1}Cs_{2.5}(VO)_{0.2}PMo_{11}VO_{40}$ and $H_{1.5}Cs_{2.5}PMo_{11}VO_{40}$ showed identical diffraction patterns as well as spectroscopic features after reaction, suggesting that the introduction of vanadium and cesium to the secondary structure of HPCs would notably increase the structure stability of the Keggin unit.

3.1.4. TPR

Fig. 4 shows the H_2-TPR results of the as-prepared samples. All of the samples showed one main reduction peak within the temperature range of 650–730 °C. Because the $Cs_{2.5}$ salt of molybdophosphoric acid decomposes above 540 °C [20,21], the reduction peaks in the 650–730 °C range may be ascribed to the reduction of free metal oxides originating from the decomposition of Keggin oxoanion, whereas the reduction peaks below 540 °C can be ascribed to the reduction of transition metal cations in the framework structure of HPCs. In terms of peak temperature, $H_{0.5}Cs_{2.5}PMo_{12}O_{40}$ is more stable than $H_{1.5}Cs_{2.5}PMo_{11}VO_{40}$. With the addition of $(VO)^{2+}$ to the secondary structure of HPCs, a small peak appeared in the temperature range of 630–650 °C, attributable to the reduction of segregated vanadium oxide entities. Note that the main reduction peaks of serial $H_{0.5-2x}Cs_{2.5}(VO)_xPMo_{12}O_{40}$ ($x = 0$–0.25) samples shifted gradually toward higher temperatures with increasing extent of $(VO)^{2+}$ addition, indicating improved thermal stability of the Keggin oxoanion. A similar phenomenon was observed over $H_{1.5}Cs_{2.5}PMo_{11}VO_{40}$ and $H_{1.1}Cs_{2.5}(VO)_{0.2}PMo_{11}VO_{40}$. As already revealed in the XRD examination, the VO^{2+} species at the secondary structure could enhance the salt feature of HPCs and, consequently, increase

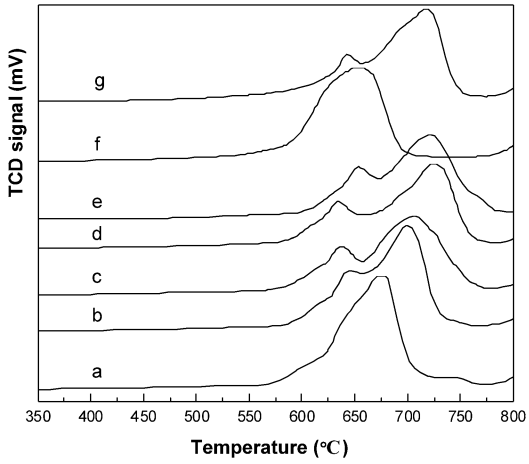

Fig. 4. Temperature-programmed reduction (TPR) profiles of the as-prepared catalysts. (a–e) $H_{0.5-2x}Cs_{2.5}(VO)_xPMo_{12}O_{40}$ ($x = 0$–0.25); (f) $H_{1.5}Cs_{2.5}PMo_{11}VO_{40}$; (g) $H_{1.1}Cs_{2.5}(VO)_{0.2}PMo_{11}VO_{40}$.

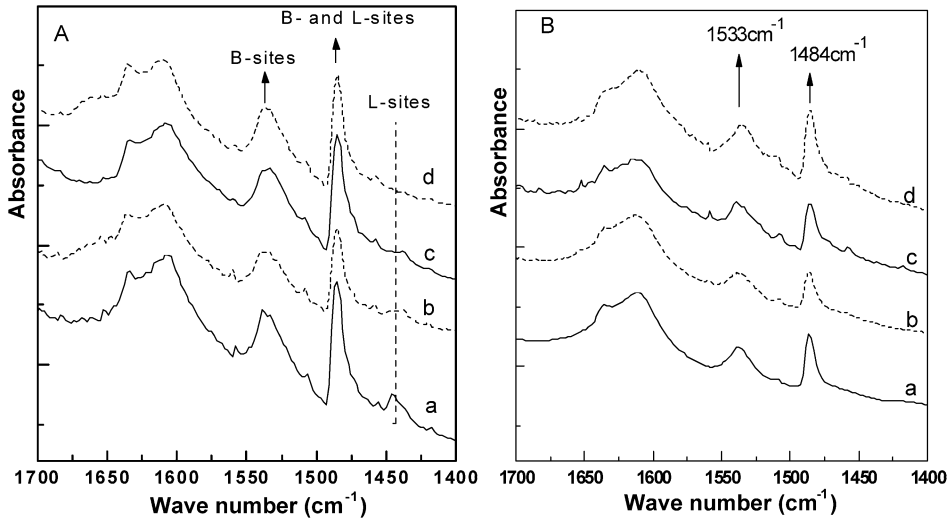

Fig. 5. Infrared spectra of pyridine adsorption on the sample surfaces. (A) Pyridine adsorption at RT (1 h) followed by 1 h evacuation at RT, and (B) heating to 160 °C and maintaining at 160 °C for 1 h. (a) $H_{0.5}Cs_{2.5}PMo_{12}O_{40}$; (b) $H_{0.1}Cs_{2.5}(VO)_{0.2}PMo_{12}O_{40}$; (c) $H_{1.5}Cs_{2.5}PMo_{11}VO_{40}$; and (d) $H_{1.1}Cs_{2.5}(VO)_{0.2}PMo_{11}VO_{40}$.

Table 1
Relative areas of the IR bands of pyridine adsorption on different acid sites

Sample	Evacuated at RT			Evacuated at 160 °C		
	1533 cm^{-1}	1484 cm^{-1}	1444 cm^{-1}	1533 cm^{-1}	1484 cm^{-1}	1444 cm^{-1}
$H_{0.5}Cs_{2.5}PMo_{12}O_{40}$	148	124	22	46	48	–
$H_{0.1}Cs_{2.5}(VO)_{0.2}PMo_{12}O_{40}$	95	87	13	33	36	–
$H_{1.5}Cs_{2.5}PMo_{11}VO_{40}$	123	125	6	54	53	–
$H_{1.1}Cs_{2.5}(VO)_{0.2}PMo_{11}VO_{40}$	116	113	–	89	74	–

the thermal stability of the Keggin oxoanion. In terms of the onset reduction temperature, the lattice oxygen of HPC samples with vanadium in the primary/secondary structure is more reactive than that with no vanadium and should be responsible for the higher activity in propane oxidation (see Table 5 later in the paper).

3.1.5. *Pyridine adsorption*

The surface acidity of representative HPCs was examined by FTIR using pyridine as a probe. Fig. 5 presents the IR spectra of pyridine adsorbed on the sample surfaces. The adsorption of pyridine was performed at room temperature; then the system was evacuated for 1 h (case A), heated to 160 °C, and evacuated at this temperature for 1 h (case B). In case A, the IR absorption band at 1444 cm^{-1} is characteristic of chemisorbed pyridine on Lewis acid sites, the band at 1533 cm^{-1} is attributable to pyridine cations on Brønsted acid sites, and the band at 1484 cm^{-1} is due to the pyridine adsorption on both acid sites. Hence the results demonstrate the presence of both Lewis and Brønsted acid sites on the catalyst surfaces. The acidity characteristics derived on the basis of the area of IR bands are given in Table 1. These data enable a rough comparison between the relative acidity of different samples. One can see that introducing VO^{2+} species to the secondary structure of HPCs (in the b and d cases) can diminish the intensity of IR bands at 1533 and 1444 cm^{-1} (especially the latter), corresponding to a reduction in surface Lewis acidity as well as Brønsted acidity. It is clear that V-substitution at the primary structure of oxoanion would cause an obvious reduction in the number of Lewis acid sites. A previous study of $H_3PMo_{12}O_{40}$ catalyst pretreated with pyridine indicated that the presence of an appropriate amount of Lewis acid sites was beneficial for AA formation [13]. On the other hand, although substituting Mo with V at the primary structure of HPCs apparently increased the number of protons, pyridine adsorption measurement indicated that the acidity of proton could vary (samples c and d). After evacuation at 160 °C for 1 h, the bands at ca. 1444 cm^{-1} essentially disappeared, whereas the weakened bands at around 1533 and 1484 cm^{-1} remained. This finding suggests that Brønsted acidity is stronger than Lewis acidity on these catalyst surfaces.

3.2. *Reaction study*

3.2.1. *Effect of Cs^+-substitution*

The Cs^+-substituted molybdophosphates were previously reported to be somewhat effective for the partial oxidation of *iso*-butane, and a maximum 3.8% MAA yield was obtained at 340 °C over a $Cs_{2.5}$-substituted sample [26]. In the present work, the effect of Cs^+-substitution in $H_{3-x}Cs_xPMo_{12}O_{40}$ on propane oxidation was investigated. As shown in Table 2, the surface area increased monotonously with the extent of Cs^+ substitution, suggesting that the texture/morphology of samples can be significantly altered. Under the adopted reaction conditions, the catalysts with different Cs content ($x = 0.0$, 1.0, 2.0, 2.5, and 3.0) demonstrated propane conversion of 2.0, 7.2, 10.1, 32.5, and 0%, respectively, and AA selectivity and yield

Table 2
Partial oxidation of propane over $H_{3-x}Cs_xPMo_{12}O_{40}$ at 400 °C[a]

x	S (BET) ($m^2\,g^{-1}$)	Conversion (%)	Selectivity (%)						AA yield (%)
			AA	ACT	ACR	AcOH	$C_3^=$	CO_x	
0.0	1.0	2.0	0.6	0.0	0.4	0.6	6.3	92.1	Trace
1.0	2.1	7.2	7.2	0.0	4.6	6.6	32.4	49.2	0.5
2.0	8.9	10.1	9.6	0.0	2.5	7.4	15.5	64.9	1.0
2.5	71.9	32.5	7.3	0.2	1.3	8.5	28.5	54.2	2.4
3.0	–	0.0	0.0	0.0	0.0	0.0	0.0	0.0	None

[a] Catalyst: 1.0 g; flow rate: 15 ml min^{-1}; feed composition: $C_3/O_2/He$ (v/v/v) = 17/30/53.
ACT: acetone; ACR: acrolein; AcOH: acetic acid; $C_3^=$: propylene.

of 0.6, 7.2, 9.6, 7.3, and 0% and 0, 0.5, 1.0, 2.4, and 0%, respectively. A maximum 2.4% AA yield was obtained at Cs content $x = 2.5$. It follows that there is a certain amount of cesium substitution that corresponds to optimal tuning of the physicochemical properties of catalyst for AA formation.

As shown in Table 2, Cs^+ substitution can change the product distribution dramatically. Introducing Cs component into the catalysts can result in a significantly reduced selectivity to carbon oxides and increased selectivity to oxygenates and propylene, plausibly as a result of altered redox character and decreased surface acidity. The color of the used $H_{3-x}Cs_xPMo_{12}O_{40}$ catalysts varied from dark green to yellowish-green, corresponding to the extent of Cs^+ substitution (from 0 to 2.5), suggesting that lesser amounts of the Mo component was reduced with gradual Cs^+ substitution. In fact, the color of $Cs_3PMo_{12}O_{40}$ remained unchanged after the reaction. Note that there is no proton and thus no Brønsted acidity in the sample of $Cs_3PMo_{12}O_{40}$; as can be seen from Table 2, this catalyst is completely inactive. It follows that substituting H^+ with Cs^+ would result in the tuning of surface acidity of the catalyst, with appropriate Brønsted sites present on the catalyst surface for the target reaction.

3.2.2. *Effect of VO^{2+}-substitution*

It was reported previously [12] that the Keggin-type HPCs prepared with H_3PO_4, MoO_3, and V_2O_5 as starting materials via the evaporation method were active for propane partial oxidation. It was presumed that some VO^{2+} as well as free V_2O_5 could be present in the catalysts. To enhance the catalytic activity and to suppress deep oxidation, further tuning of the catalyst properties by adding vanadium component at the secondary structure of HPC was investigated for propane oxidation.

The effect of VO^{2+} substitution in $H_{0.5-2x}Cs_{2.5}(VO)_xPMo_{12}O_{40}$ on propane oxidation is depicted in Table 3. The conversion was 24.2, 36.1, 36.6, 40.6, and 39.5% at $x = 0.0$, 0.10, 0.15, 0.20, and 0.25, respectively, and the selectivity and yield of AA were 7.8, 19.5, 21.9, 20.3, and 17.4% and 1.9, 7.0, 8.0, 8.2, and 6.9%, respectively. The highest AA yield of 8.2% was obtained at $x = 0.20$. The substitution of VO^{2+} at the secondary structure notably enhanced the overall propane conversion and also considerably increased the AA selectivity, as shown in Table 3. It also noticeably suppressed propylene formation, but did not significantly alter the selectivity to acetic acid (AcOH) and carbon oxides (CO_x). It seems that the

Table 3
Propane oxidation over $H_{0.5-2x}Cs_{2.5}(VO)_xPMo_{12}O_{40}$ at 420 °C[a]

x	Conversion (%)	Selectivity (%)					AA yield (%)
		AA	ACR	AcOH	$C_3^=$	CO_x	
0.00	24.2	7.8	1.8	4.2	11.6	74.6	1.9
0.10	36.1	19.5	1.0	4.5	3.5	71.5	7.0
0.15	36.6	21.9	1.0	4.7	3.6	68.8	8.0
0.20	40.6	20.3	0.9	4.5	3.6	70.8	8.2
0.25	39.5	17.4	0.9	4.4	3.4	73.8	6.9

[a] Catalyst: 1.0 g; flow rate: 15 ml min^{-1}; feed composition: $C_3/O_2/He$ (v/v/v) = 10/20/70.

Table 4
Partial oxidation of propane over heteropolyacids with different vanadium locations at 400 °C[a]

Catalyst	Conversion (%)	Selectivity (%)					AA yield (%)
		AA	ACR	AcOH	$C_3^=$	CO_x	
$H_3PMo_{12}O_{40}$	2.0	0.6	0.4	0.6	6.3	92.1	Trace
$H(VO)PMo_{12}O_{40}$	52.7	4.9	0.2	7.9	1.9	85.1	2.6
$H_4PMo_{11}VO_{40}$	13.3	2.9	2.2	3.7	58.9	32.3	0.4

[a] Catalyst: 1.0 g; flow rate: 15 ml min^{-1}; feed composition: $C_3/O_2/He$ (v/v/v) = 17/30/53.

promotion of propane oxidation to AA is feasible via VO^{2+} substitution at the secondary structure. It has been suggested that the possible reaction route from propane to AA follows propane → propylene → acrolein → AA [18], and that the $(VO)^{2+}$-modified HPCs can effectively promote the conversion of propylene (in lesser amounts among the final products) to acrolein and further to AA, which are the rate-determining steps for the overall reaction. As discussed above, the outcomes of XRD and TPR investigations revealed that an appropriate extent of VO^{2+} substitution ($x \geqslant 0.2$) at the secondary structure of HPC could stabilize the oxoanions as well as the whole structure of HPC. No free MoO_3 and V_2O_5 phases were detected by XRD after the reaction.

3.2.3. *Effect of vanadium location*

To gain a better understanding of the effect of vanadium substitution in HPC on propane oxidation, the effect of introducing vanadium into the primary or the secondary structure of pure HPAs on catalytic activity was studied. The results, given in Table 4, demonstrate that propane conversion was very low on $H_3PMo_{12}O_{40}$ and only a trace amount of AA was produced. Introducing vanadium (one vanadium atom per oxoanion) into the secondary structure of HPA caused an abrupt increase in propane conversion with certain enhancement in AA selectivity. With vanadium added in the primary structure, there was only a slight increase in propane conversion and AA selectivity, but a significant increase in propylene selectivity (up to 58.9%). The results demonstrate that introducing vanadium species to the secondary structure of HPA is beneficial for AA formation.

To further clarify the role of vanadium component in heteropoly compounds for propane oxidation, the effect of adding vanadium species at the primary (Keggin anion) and/or the secondary structure of the cesium salts of HPAs on catalytic activity was studied. The results are provided in Table 5. The

Table 5
Partial oxidation of propane over the cesium salts of heteropolyacids with different vanadium locations at 420 °C[a]

Catalyst	Conversion (%)	Selectivity (%)					AA yield (%)
		AA	ACR	AcOH	$C_3^=$	CO_x	
$H_{0.5}Cs_{2.5}PMo_{12}O_{40}$	24.2	7.8	1.8	4.2	11.6	74.6	1.9
$H_{0.1}Cs_{2.5}(VO)_{0.2}PMo_{12}O_{40}$	40.6	20.3	0.9	4.5	3.6	70.8	8.2
$H_{1.5}Cs_{2.5}PMo_{11}VO_{40}$	46.2	2.0	0.5	1.8	2.8	93.0	0.9
$H_{1.1}Cs_{2.5}(VO)_{0.2}PMo_{11}VO_{40}$	43.6	5.3	0.6	3.1	4.2	86.8	2.3

[a] Catalyst: 1.0 g; flow rate: 15 ml min^{-1}; feed composition: C_3/O_2/He (v/v/v) = 10/20/70.

$H_{1.5}Cs_{2.5}PMo_{11}VO_{40}$ catalyst with one vanadium atom at the primary structure exhibited notably enhanced activity but significantly diminished selectivity to oxygenates and propylene. Further addition of vanadium species ($x = 0.2$) to the secondary structure caused a slight decrease in activity and an increase in AA selectivity. It follows that coexistence of $(VO)^{2+}$ and Cs^+ at the secondary structure with the oxoanion unit would result in a synergetic effect that is beneficial for enhanced AA selectivity. The substitution of Mo^{6+} with V^{5+} in the Cs salts of HPAs would result in the generation of more reactive lattice oxygen associated to the Mo–O–V species, consistent with the trend observed over the non-Cs-substituted HPAs (data shown in Table 4).

The reaction data of the present study demonstrate that an appropriate amount of $(VO)^{2+}$ at the secondary structure of HPC is critical for propane activation and AA formation. Actually, vanadium is a basic catalyst component effective for propane oxidative dehydrogenation (ODH) to propylene [27–30], as well as for propane oxidation to AA over VPO and Mo–V–Te(Sb)–Nb MMO catalysts [31–38]. We propose that small amount of segregated vanadium oxide species outside the Keggin structure of HPC might have a function similar to that of $(VO)^{2+}$ at the secondary structure of HPC, inducing a synergistic effect with the oxoanion unit and producing an affirmative outcome for propane oxidation to AA. The presence of segregated vanadium oxide species might somehow modify the redox properties of HPCs and consequently change the catalyst behavior.

3.2.4. *Effect of operation variables*

The effects of operation variables, including reaction temperature, feed composition, and the presence of steam on catalyst behavior, were also studied.

3.2.4.1. Reaction temperature The temperature dependence of reaction performance over $H_{0.1}Cs_{2.5}(VO)_{0.2}PMo_{12}O_{40}$ is shown in Fig. 6. The propane conversion increased monotonously at elevated temperatures in the 360–430 °C region. The selectivity to acetone and acrolein was rather low (<5%) in the whole temperature range, because these were intermediate products and were readily oxidized to CO_x [31,33]. The selectivity to propylene decreased rapidly with temperature rise, indicating that it is a key intermediate quickly consumed in the "next-step" reaction. The selectivity to AA increased gradually with increasing temperature, reaching a maximum value of 31.5% at 420 °C. In contrast, the selectivity to acetic acid declined notably with increasing temperature. Similar temperature dependence of the selectivity of acetic acid and AA was also observed over a Mo–V–Sb–Nb catalyst [35], probably due to the different formation kinetics of the acids [35]. Over the aforementioned MMO catalyst, the apparent activation energy of AA formation (23 kJ mol^{-1}) is much higher than that of acetic acid formation (3 kJ mol^{-1}); thus high temperature (>683 K) is favorable for better selectivity to AA. On the other hand, the reactivity of such products as acetic acid and AA could vary over different catalysts [31,33]. It was reported that acetic acid was more reactive than AA over the VPO-type catalysts [31]. In the present study, the formation of AA is temperature-dependent and probably kinetically controlled over the HPC-type catalysts. The highest AA selectivity was usually achieved at ca. 420 °C over the HPC catalysts. Thus the comparison of reaction performance with respect to feed composition and water vapor was made in the temperature range 400–430 °C (Tables 6 and 7).

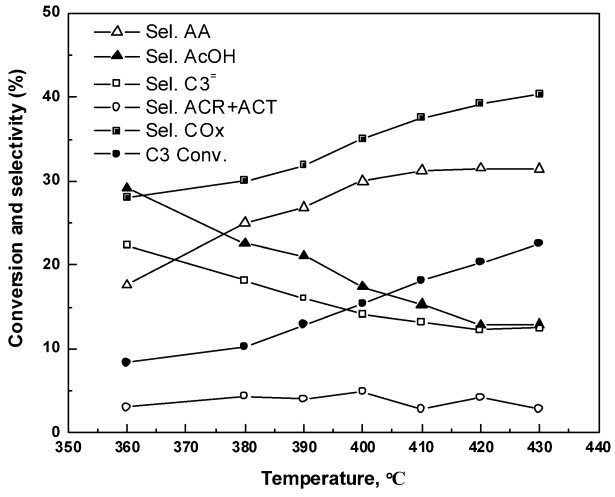

Fig. 6. Temperature dependence of reaction performance over $H_{0.1}Cs_{2.5}(VO)_{0.2}PMo_{12}O_{40}$ catalyst. Feed composition: C_3/O_2/He/H_2O (v/v/v/v) = 14/7/49/30.

Table 6
Propane partial oxidation over $H_{0.1}Cs_{2.5}(VO)_{0.2}PMo_{12}O_{40}$ in different feeds[a]

Gas composition (C_3/O_2/He)	T (°C)	Conversion (%)	Selectivity (%)					AA yield (%)
			AA	ACR	AcOH	$C_3^=$	CO_x	
10/20/70	400	38.6	18.6	0.8	6.7	3.0	71.0	7.2
	420	40.6	20.3	0.9	4.5	3.6	70.8	8.2
20/10/70	400	24.1	21.8	1.8	11.3	16.2	48.9	5.3
	420	26.7	26.0	1.9	9.8	12.2	50.1	6.9

[a] Catalyst: 1.0 g; flow rate: 15 ml min^{-1}.

Table 7
Propane partial oxidation over $H_{0.1}Cs_{2.5}(VO)_{0.2}PMo_{12}O_{40}$ in the presence of steam[a]

Gas composition ($C_3/O_2/He/H_2O$(g))	T (°C)	Conversion (%)	Selectivity (%)					AA yield (%)
			AA	ACR	AcOH	$C_3^=$	CO_x	
7/14/49/30	420	26.9	24.3	1.4	12.6	5.7	55.9	6.5
	430	29.7	20.1	1.7	10.8	7.8	59.6	6.0
14/7/49/30	420	20.3	31.5	4.2	12.8	12.3	39.2	6.4
	430	22.5	31.4	2.8	12.9	12.5	40.4	7.1

[a] Catalyst: 1.0 g; flow rate: 15 ml min^{-1}.

3.2.4.2. Feed composition The catalytic reactions over $H_{0.1}Cs_{2.5}(VO)_{0.2}PMo_{12}O_{40}$ were performed in both oxygen-rich and hydrocarbon-rich atmospheres; the results are given in Table 6. The catalyst was more active but less selective to AA in an oxygen-rich atmosphere. The oxygen-rich atmosphere understandably suppressed propylene formation but enhanced deep oxidation to carbon oxides.

The partial oxidation of propane over VPO-type catalysts was performed mostly under oxygen-rich conditions. Mota et al. reported the deactivation of VPO catalyst under hydrocarbon-rich conditions, as well as the ability of certain dopants, such as cobalt, to restore catalyst activity [39]. The catalysis of MMOs was usually performed under oxygen-rich conditions, with the reoxidation step considered one of the rate-determining steps [40].

3.2.4.3. Water vapor It is generally recognized that water vapor (steam) can play an important role in propane partial oxidation; its presence can cause a significant improvement in oxygenate selectivity [13,15,31–37]. In this study, 30% (by volume) of water vapor was introduced into the reaction system; the reaction data are given in Table 7. The presence of steam caused a reduction in propane conversion and an increase in AA selectivity with a notable drop in CO_x formation under both oxygen-rich and hydrocarbon-rich conditions. Note that acetic acid formation increased notably in the presence of water under oxygen-rich conditions (Tables 6 and 7), suggesting a possible shift in the reaction mechanism. The mechanism for propane partial oxidation has been widely discussed in the literature [21,31,35,36]. The reaction pathway of propane oxidation over the present HPC catalysts is thought to be similar to that suggested for the $Cs_{2.5}H_{1.5}PV_1W_xMo_{11-x}O_{40}$ catalysts [41]. As seen in Scheme 1, the reaction route of propane first ODH to propylene then to acrolein and eventually to AA is the well-known pathway for AA formation from propane. Water presence can favor the route of propylene hydration to isopropyl alcohol, then dehydrogenation to acetone and further oxidation to acetic acid and CO_x. The influence of water on acetic acid formation has been observed over HPC-type [12,15,21,41] and VPO-type catalysts [31,32], as well as over the Mo–V–Te(Sb)–Nb catalysts [34–36].

The hydration of propylene to isopropyl alcohol is an acid-catalyzed reaction, and the formation of acetic acid is closely related to the strong Brønsted acid sites present on the catalyst surface [21,35,36,42]. In a dehydroxylation process, the

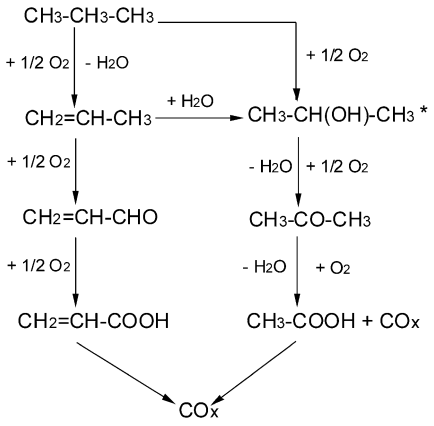

Scheme 1. The reaction mechanism suggested for propane oxidation over HPC-type catalyst. The asterisk denotes that the proposed compound has not been detected experimentally [41].

protons can be removed in the form of constitutional water, and the Brønsted acid sites of HPC will be eliminated under reaction conditions, leading to rather low selectivity to acetic acid [21]. By adding water to the feed gas, the acidic feature as well as the Keggin structure of HPC can be largely maintained, giving rise to enhanced selectivity of oxygenates [15,21,43,44]. Water can also promote desorption of the acidic products (AA and acetic acid) and remove the reaction heat from catalyst bed, preventing the deep oxidation of products. The role of water may vary over different catalyst systems. On the VPO-type catalysts, the effect of water is attributed to the enhanced crystallinity of the $(VO)_2P_2O_7$ phase, suppression of the formation of V^{5+}-containing species, and maintenance of an appropriate distribution of surface acid sites [32]. Over the Mo–V–Sb–Nb mixed-oxide catalysts, water vapor stabilizes certain active phases and lowers the activation energy of the propane oxidation reaction [35,36].

4. Conclusion

In this study we have demonstrated that vanadium substitution at the primary/secondary structures of HPCs can significantly affect catalyst performance. Introducing vanadium at the primary structure (Keggin anion) of molybdophosphates can enhance the catalytic activity, and a small fraction of vanadium can be segregated in the form of free V_2O_5 during the reaction. The addition of vanadium species to the secondary structure can result in a much more active and selective catalyst for AA production. The highest AA yield was obtained over $H_{0.1}Cs_{2.5}(VO)_{0.2}PMo_{12}O_{40}$ at an optimal reaction temperature of 420 °C. The enhanced catalytic performance with respect to $(VO)^{2+}$ addition at the HPC secondary structure can be attributed to the possible synergism among vanadium species, oxoanion, and cesium entities, as well as to the resulting modified surface acidity, structural stability, and redox properties. Small amounts of segregated vanadium oxide species outside the Keggin structure may function similarly as $(VO)^{2+}$ at the HPC secondary structure. An excess amount of oxygen in the reaction system would increase propane conversion, but reduce AA and propylene selectivity. On the other hand, the presence

of steam noticeably suppressed deep oxidation and enhanced AA and acetic acid formation.

Acknowledgments

Financial support from the Ministry of Science and Technology of China (grant 2000048009), Rohm & Haas, and BASF is gratefully acknowledged.

References

[1] F. Cavani, F. Trifiro, Catal. Today 51 (1999) 561.
[2] N. Mizuno, M. Misono, Chem. Rev. 98 (1) (1998) 199.
[3] M. Baerns, O. Buyevskaya, Catal. Today 45 (1998) 13.
[4] K. Bruckman, J. Haber, in: New Frontiers in Catalysis, Proceedings of the 10th International Congress on Catalysis, Budapest, Hungary, 1993, p. 741.
[5] F. Cavani, M. Koutyrev, F. Trifiro, Catal. Today 24 (1995) 365.
[6] W. Li, W. Ueda, Catal. Lett. 46 (1997) 261.
[7] G. Busca, F. Cavani, E. Etienne, E. Finocchio, A. Galli, G. Selleri, F. Trifiro, J. Mol. Catal. A 114 (1996) 343.
[8] F. Cavani, E. Etienne, M. Favaro, A. Galli, F. Trifirò, G. Hecquet, Catal. Lett. 32 (1995) 215.
[9] D. Casarini, G. Centi, P. Jiru, V. Lena, Z. Tvaruzkova, J. Catal. 143 (1993) 325.
[10] M. Ai, J. Catal. 85 (1984) 324.
[11] X. Mao, Y.Q. Yin, B.K. Zhong, H. Wang, X.H. Li, J. Mol. Catal. A 169 (2001) 199.
[12] H.S. Jiang, X. Mao, S.J. Xie, B.K. Zhong, J. Mol. Catal. A 185 (2002) 143.
[13] W. Li, K. Oshihara, W. Ueda, Appl. Catal. A 182 (1999) 357.
[14] N. Mizuno, M. Tateishi, M. Iwamoto, Appl. Catal. A 128 (1995) L165.
[15] J.H. Holles, C.J. Dillon, J.A. Labinger, M.E. Davis, J. Catal. 218 (2003) 42.
[16] X.K. Li, Y. Lei, Q. Jiang, J. Zhao, W.J. Ji, Z.B. Zhang, Y. Chen, Acta Chim. Silica 63 (2005) 1049.
[17] X.K. Li, Y. Lei, J. Zhao, W.J. Ji, Z.B. Zhang, Y. Chen, Chem. J. Chin. Univ. 26 (2005) 1716.
[18] M.M. Lin, Appl. Catal. A 207 (2001) 1.
[19] G. Centi, F. Trifiro, Selective Oxidation of Light Alkanes: Comparison between Vanadyl Pyrophosphate and V-Molybdophosphoric Acid, in: Catal. Sci. Technol., Proc. Tokyo Conf., 1st Meeting, 1991, pp. 225–230.
[20] N. Mizuno, D.J. Sun, W. Han, T. Kudo, J. Mol. Catal. A 114 (1996) 309.
[21] N. Dimitratos, J.C. Védrine, Appl. Catal. A 256 (2003) 251.
[22] S. Karmakar, F.A. Volpe Jr., E.P. Ellis Jr., E.J. Lyons, US Patent 6,043,184 (2000).
[23] M.T. Pope, Heteropoly and Isopoly Oxometalates, Springer, New York, 1983.
[24] F. Cavani, A. Tanguy, F. Trifiro, M. Koutrev, J. Catal. 174 (1998) 231.
[25] M. Langpape, J.M.M. Millet, U.S. Ozkan, M. Boudeulle, J. Catal. 181 (1999) 80.
[26] N. Mizuno, M. Tateishi, M. Iwamoto, J. Catal. 163 (1996) 87.
[27] Y.M. Liu, Y. Cao, K.K. Zhu, S.R. Yan, W.L. Dai, H.Y. He, K.N. Fan, Chem. Commun. (2003) 2832.
[28] Y.M. Liu, Y. Cao, S.R. Yan, W.L. Dai, K.N. Fan, Catal. Lett. 88 (2003) 21.
[29] A. Khodakov, B. Olthof, A.T. Bell, E. Iglesia, J. Catal. 181 (1999) 205.
[30] M.A. Chaar, D. Patel, H.H. Kung, J. Catal. 109 (1988) 463.
[31] M. Ai, J. Catal. 101 (1986) 389.
[32] G. Landi, L. Lisi, J.C. Volta, J. Mol. Catal. A 222 (2004) 175.
[33] M. Lin, T.B. Desai, F.W. Kaiser, P.D. Klugherz, Catal. Today 61 (2000) 223.
[34] B. Zhu, H. B Li, W.S. Yang, L.W. Lin, Catal. Today 93–95 (2004) 229.
[35] E.K. Novakova, E.G. Derouane, J.C. Védrine, Catal. Lett. 83 (2002) 177.
[36] E.K. Novakova, J.C. Védrine, E.G. Derouane, J. Catal. 211 (2002) 226.
[37] E.K. Novakova, J.C. Védrine, E.G. Derouane, J. Catal. 211 (2002) 235.
[38] M.M. Lin, Appl. Catal. A 250 (2003) 305.
[39] S. Mota, M. Abon, J.C. Volta, J.A. Dalmon, J. Catal. 193 (2000) 308.
[40] E. Balcells, F. Borgmeier, I. Grißtede, H.G. Lintz, F. Rosowski, Appl. Catal. A 266 (2004) 211.
[41] N. Nikos, J.C. Védrine, in: S.D. Jackson, J.S.J. Hargreaves, D. Lennon (Eds.), Applied Catalysis, Royal Society Chemistry of Great Britain, London, 2003.
[42] M. Ai, Catal. Today 13 (1992) 679.
[43] C.J. Dillon, J.H. Holles, R.J. Davis, J.A. Labinger, M.E. Davis, J. Catal. 218 (2003) 42.
[44] N. Essayem, Y. Tong, H. Jobic, J.C. Védrine, Appl. Catal. A 194 (2000) 109.